Electronic Supplementary Material (ESI) for Analyst.

Electronic Supplementary Information

to

Quantitative analysis of biochemical processes in living cells at a single-molecule level: a case of olaparib-PARP1 (DNA repair protein) interactions

Aneta Karpińska, Marta Pilz, Joanna Buczkowska, Paweł J. Żuk, Karolina Kucharska, Gaweł Magiera, Karina Kwapiszewska, Robert Hołyst

ESI1. MDA-MB-231 oncosomes

Confocal images of Triple-Negative Breast Cancer (TNBC) cells after the uptake of the olaparib analog, presented in Fig. S1A, showed the presence of oncosomes, extracellular vesicles characteristic for cancer cells.

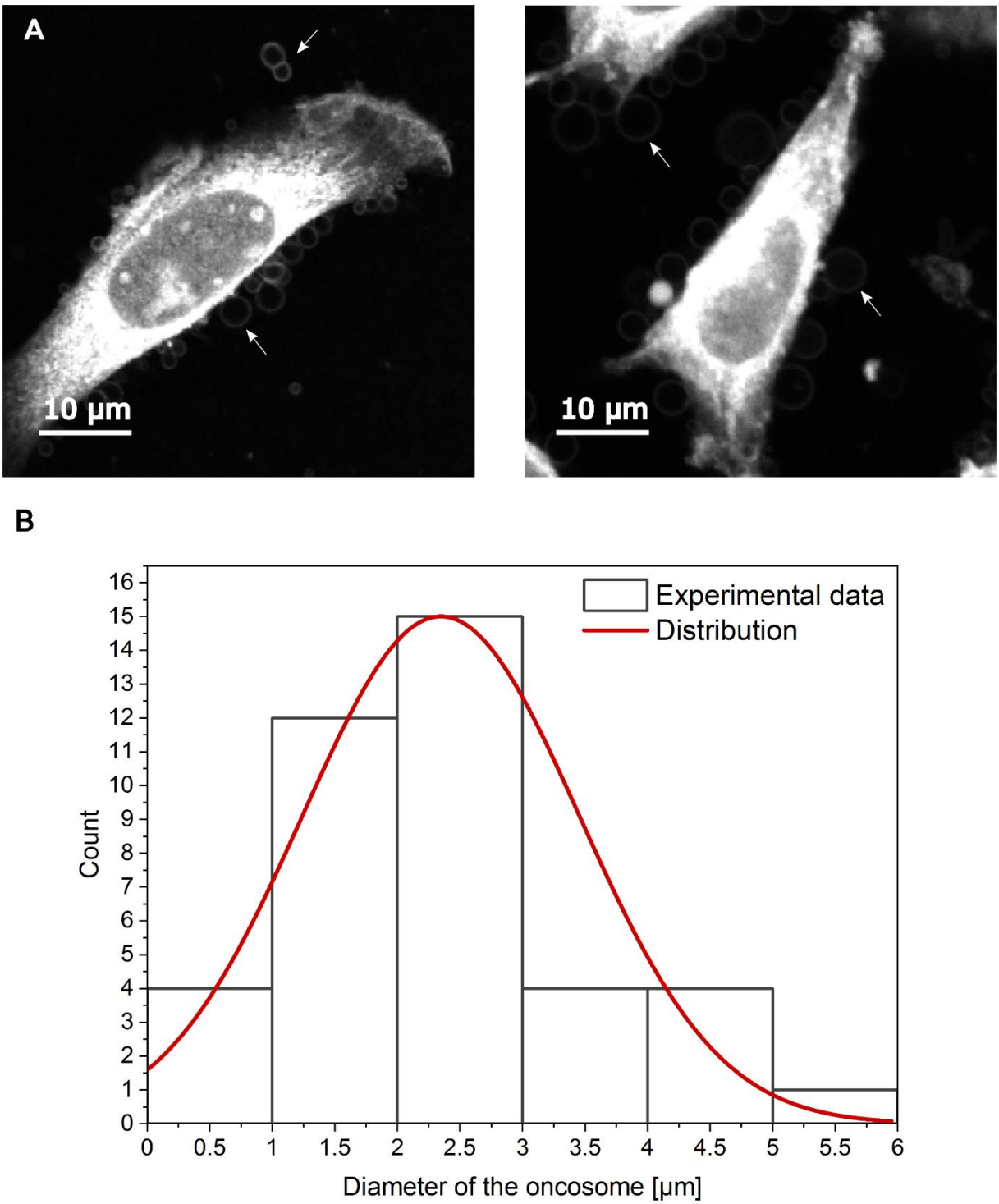

Fig. S1 Confocal imaging of TNBC with oncosome analysis. (A) Confocal images of MDA-MB-231 cells with oncosomes around. Arrows indicate examples of oncosomes. (B) Histogram of TNBC cells oncosomes diameter with the distribution line.

The oncosomes diameters of the MDA-MB-231 cell line, calculated from the confocal images shown above, are summarized as a histogram (Fig. S1B). It revealed that the most common vesicle size is about 2.25 µm in diameter.

Slightly smaller oncosomes (about 1.5 µm in diameter) were also abundant. The largest vesicle size was 5.3 µm. The obtained results are in good agreement with literature data.[17]

ESI2. 3D imaging

3D imaging showed that the olaparib derivative penetrates the MDA-MB-231 spheroid in less than 25 min. For a more detailed analysis, we performed a surface intensity analysis based on a section of the spheroid at a depth of 25 µm (Fig. S2).

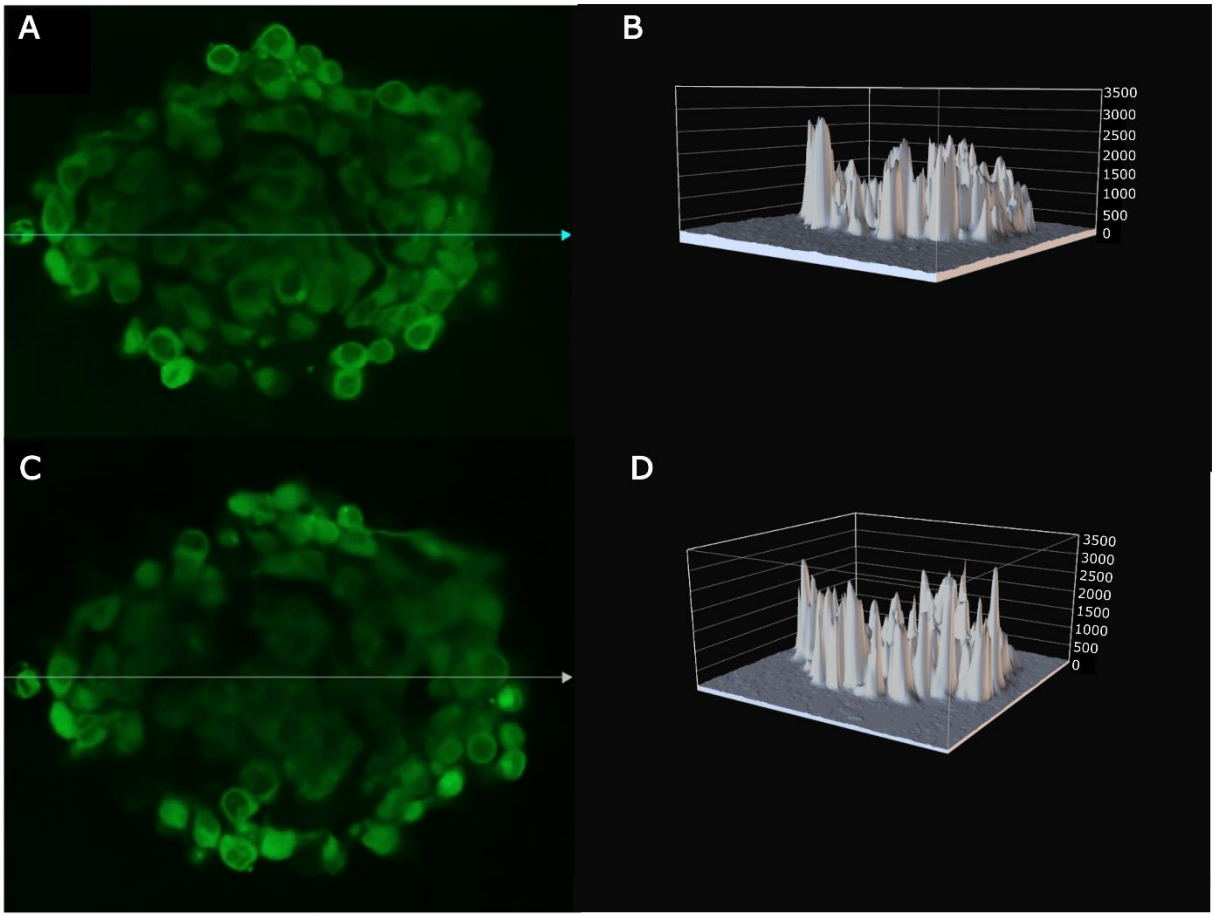

Fig. S2 Analysis of PARPi-FL intensity in MDA-MB 231 spheroid depending on incubation time. (A,B) Cross-section of a spheroid at a depth of 25 µm and the three dimensional surface plot of PARPi-FL fluorescence intensity (in arbitrary units) immediately after adding the compound to the medium. (C,D) Cross-section of a spheroid at a depth of 25 µm and the three dimensional surface plot of PARPi-FL fluorescence intensity after 25 min of incubation.

The fluorescence intensity analysis performed allows us to see slight differences in the penetration of PARPi-FL into MDA-MB 231 spheroid cells depending on the incubation time of the inhibitor with spheroids. Nevertheless, olaparib penetration occurs rapidly and does not change after time.

ESI3. The partition coefficient of HeLa and MDA-MB231 cells under 2D and 3D culture conditions

We presented differences at the quantitative level in the penetration of the olaparib analog into TNBC and Cervical Cancer (CC) cells as a partition coefficient. This parameter is the ratio of the inhibitor concentration inside the cells to its concentration in the culture medium. We determined the partition coefficient for cells cultured as a monolayer (2D) and in the form of spheroids - 3D. For each variant, 3-4 different concentrations were tested. The results of measured concentrations in the medium and inside the cells, as well as partition coefficient calculated on their basis, are presented in Table S1.

Table S1. Overview of partition coefficients for MDA-MB 231 and HeLa cells cultured in 2D and 3D growth conditions concerning medium and intracellular concentrations. Errors were calculated using total differential method (number of tested cells N = 12; each cell was measured three times).

C_{medium} 2D [nmol/L]	C_{cell} 2D [nmol/L]	Partition coefficient
MDA-MB-231 2D growth conditions		
69.90 ± 16.80	452.81 ± 108.85	6.48 ± 2.20
28.02 ± 6.74	191.81 ± 46.11	6.85 ± 2.33
5.64 ± 1.35	34.35 ± 8.26	6.09 ± 2.07
2.20 ± 0.53	37.92 ± 9.12	8.24 ± 2.77
MDA-MB-231 3D growth conditions		
40.28 ± 9.68	614.13 ± 147.64	15.25 ± 5.18
27.26 ± 5.87	377.70 ± 81.33	13.86 ± 4.22
10.33 ± 2.22	143.63 ± 30.93	13.90 ± 4.23
HeLa 2D growth conditions		
65.53 ± 15.62	613.15 ± 147.40	9.36 ± 3.17
29.01 ± 6.91	339.43 ± 81.59	11.70 ± 3.96
12.96 ± 3.09	108.69 ± 26.13	8.39 ± 2.84
19.67 ± 4.69	133.35 ± 32.06	6.78 ± 2.30
HeLa 3D growth conditions		
22.40 ± 5.81	540.51 ± 129.94	24.13 ± 8.53
11.02 ± 2.63	254.10 ± 61.08	23.06 ± 7.81
6.58 ± 1.57	153.77 ± 36.97	23.37 ± 7.92

ESI4. Cytotoxicity assays of PARPi-FL for MDA-MB-231 and HeLa cells

Before viability assays, we estimated the optimal number of cells per milliliter. It was 10^4 cells/ml for TNBC cells and $5{\cdot}10^4$/ml for HeLa cells. Measurements were performed in 96-well plates.

IC_{50} values were read directly from function plots fitted to cell viability measurement points after incubation with PARPi-FL compound in the concentration range of 0.625-160 µmol/L for MDA-MB-231 cells and 0.156-160 µmol/L for HeLa cells. The concentrations of the compound at which cell growth was inhibited by 50% (IC_{50}), obtained using MTT and alamarBlue® assays, for MDA-MB-231 and HeLa cells are summarized in Table S2. The IC_{50} concentration values are nearly 3-fold and 7-fold higher for CC than those for MDA-MB-231 based on the MTT and alamarBlue® assay, respectively.

The obtained IC_{50} values are similar for both assays. The observed differences are because the used cytotoxicity assays examine other metabolic pathways that are differently related to the crucial processes for the tested inhibitor.

Table S2. IC_{50} concentrations for MDA-MB-231 and HeLa cell lines determined by two independent cytotoxicity assays: MTT and alamarBlue®.

Cell line	IC_{50} from MTT assay [µmol/L]	IC_{50} from alamarBlue® assay [µmol/L]
MDA-MB-231	2.09	1.01
HeLa	5.49	6.73

ESI5. Cytoplasm nanoviscosity of HeLa and MDA-MB-231 cells

Information about the nanoviscosity of the compartment of the cell in which the measurement is carried out is essential to precisely identify the components of FCS autocorrelation curves obtained in living cells. For this purpose, our team developed a length scale-dependent nanoviscosity model, described by Equation 11. The

values of each parameter for both tested cell lines (HeLa and MDA-MB-231) are presented in Table S3. Prior FCS measurement, different probes were introduced (TRITC-labeled dextrans, nanospheres, EGFP) into the cell interior (nucleus or cytoplasm) by using microinjections or Cell-IN product (in the case of MDA-MB-231). Then, for each probe, we determined their intracellular diffusion coefficients.[3,5]

Table S3. Parameter values of the scale-dependent nanoviscosity equation for the HeLa and MDA-MB-231 cell lines. Errors were calculated using total differential method (number of tested cells N = 10; each cell was measured three times).

The parameter symbol	HeLa[3]	MDA-MB-231
A	1.3 (was set)	1.3 (was set)
ξ	3.16 ± 0.14	1.70 ± 0.29
R_H	12.9 ± 2.3	2.85 ± 0.92
a	0.62 ± 0.07	0.55 ± 0.15

ESI6. Hydrodynamic radii of olaparib analog (PARPi-FL) and the complex of inhibitor and PARP1 protein

Before measurements in living cells, we performed experiments in a buffer to determine the size of two probes: PARPi-FL and a complex composed of PARP1 protein and inhibitor. These data were used to precisely identify the components detected inside the cells. The determined hydrodynamic radii of the mentioned probes, and corresponding diffusion coefficients, are presented in Table S4.

Table S4. The diffusion coefficients and hydrodynamic radii values of the olaparib analog alone, PARP1 – olaparib analog complex and olaparib analog – PARP1 – RNA complex. Errors were calculated using total differential method (number of single measurements N = 15).

Component	The diffusion coefficient in PBS solution [$\mu m^2/s$]	The predicted diffusion coefficient in the nucleus [$\mu m^2/s$][4]	Hydrodynamic radius [nm]
Olaparib analog	538.96 ± 16.63	249.85	0.56 ± 0.02
PARP1 – olaparib analog	42.10 ± 5.51	9.10	7.17 ± 0.94
olaparib analog – PARP1 protein – RNA	5.29 ± 0.60	0.99	57.10 ± 6.51

Experimental data were fitted with a one-component normal diffusion model for the PARPi-FL probe (Fig. S3A) and a two-component normal diffusion model for the PARP1 – olaparib analog complex. The first component was the freely diffusing PARPi-FL while the second component was the protein – inhibitor complex (Fig. S3B).

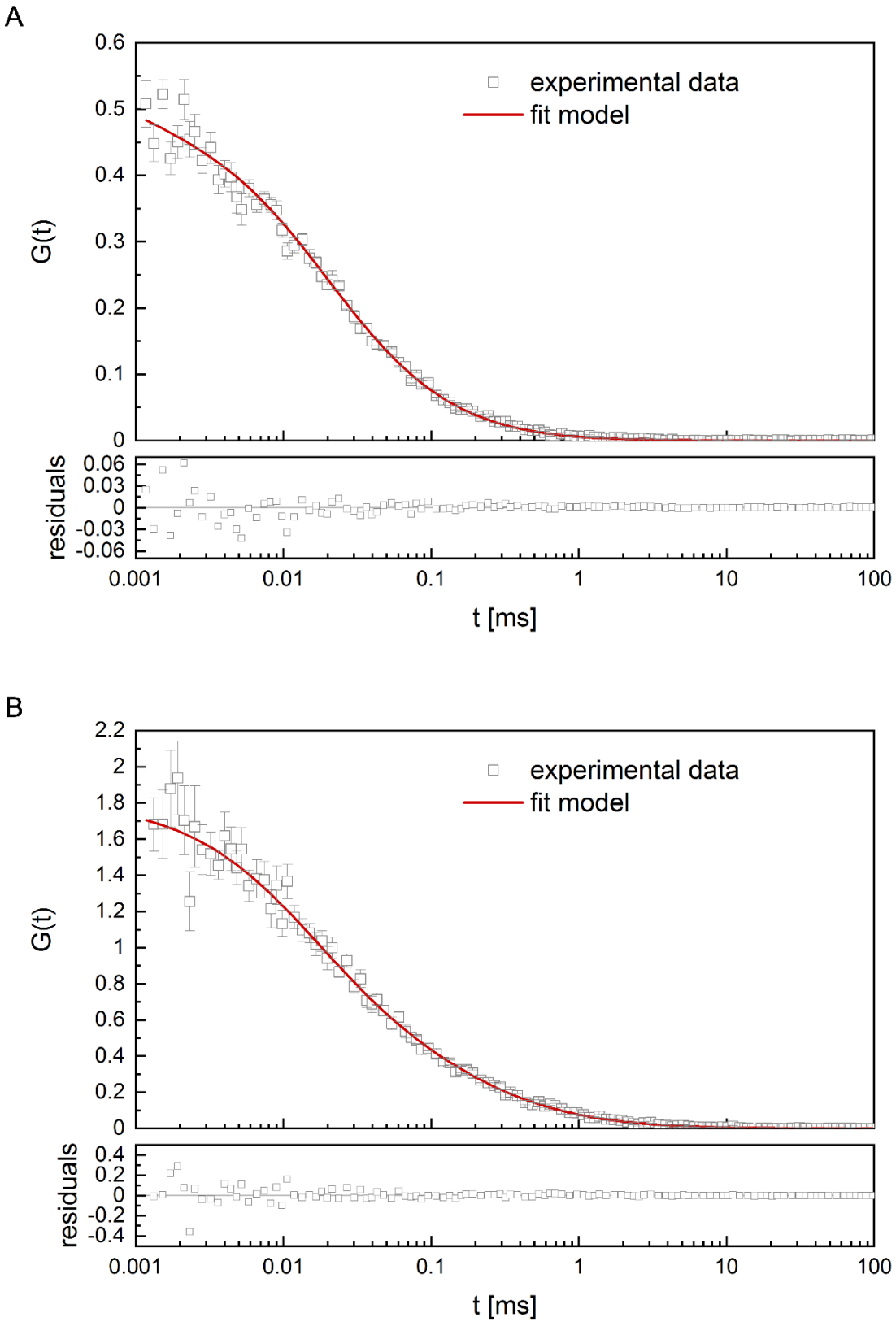

Fig. S3 FCS autocorrelation curves for olaparib analog alone and in complex with PARP1 protein. (A) FCS autocorrelation curve for the PARPi-FL probe. Experimental data were fitted with a one-component normal diffusion model (Equation 1, when i=1). (B) FCS autocorrelation curve for the PARP1 – olaparib analog complex. Experimental data were fitted with a two-component normal diffusion model (Equation 1, when i=2). The fast

fraction of molecules we identified as the freely diffusing inhibitor. For both graphs, the bottom panel shows the residual curve.

ESI7. GRPY method for determining the hydrodynamic radius of PARP1 protein

The protein PARP1, which is not connected to the DNA, is partially unstructured (Fig. S5).[30] To calculate the diffusion coefficient of such structure we a model with geometric features and the dynamics of the protein. The protein consists of six globular units linked with unstructured linkers. We assume that each of the well-structured units is a sphere having a hydrodynamic radius calculated with the GRPY method for determining hydrodynamic properties of rigid macromolecules.[34] The subunit structures, their RSCB-PDB codes, and hydrodynamic radii are summarized in Table S5. We take the shapes of subunits as they appear in the first deposited configuration in the PDB entry. Other choices are possible, e.g. the average over deposited structures, which can have some influence on the final results. The subunits are connected with flexible and approximately inextensible linkers of length l_i, different for each linker i. The length of linkers based on the protein structure is summarized in Table S6. They are equal to the sum of sphere's radii and the length of the unstructured protein chain between the well-structured segments.

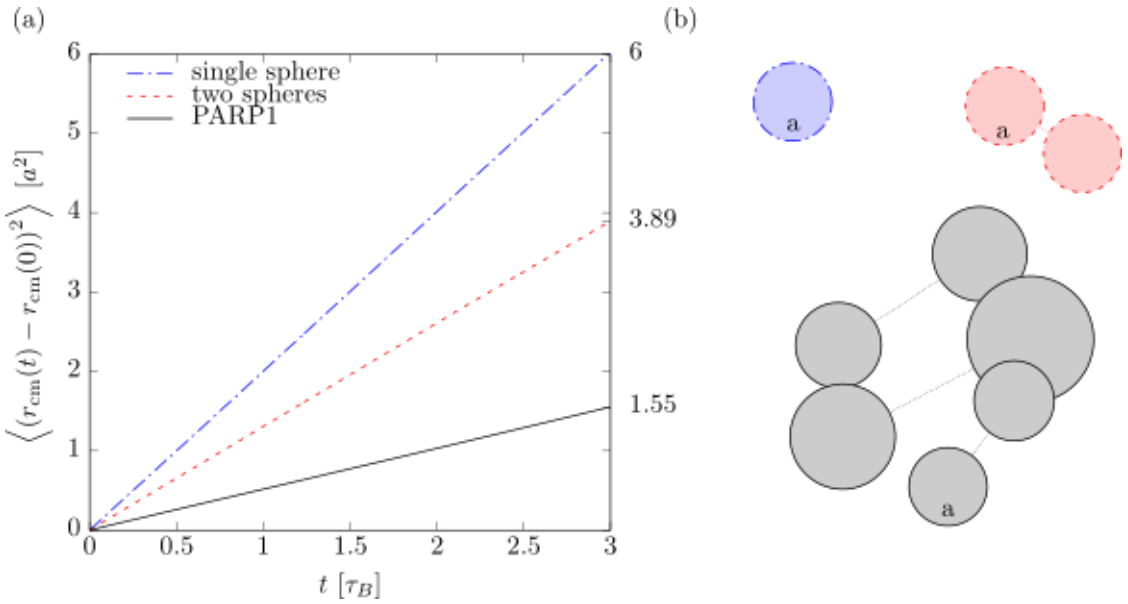

Fig. S4 Diffusion of complex non-rigid particles. (a) Simulated mean square displacement for a single sphere with radius a, dumbell with spheres of radius a that are connected with a flexible linker of length l = 4a center to center, PARP1 protein modelled with a set of spheres (smallest sphere's radius a) connected with flexible linkers. (b) 2D projection of the sphere, dumbbell, and PARP1 protein obtained from Brownian dynamics simulations.

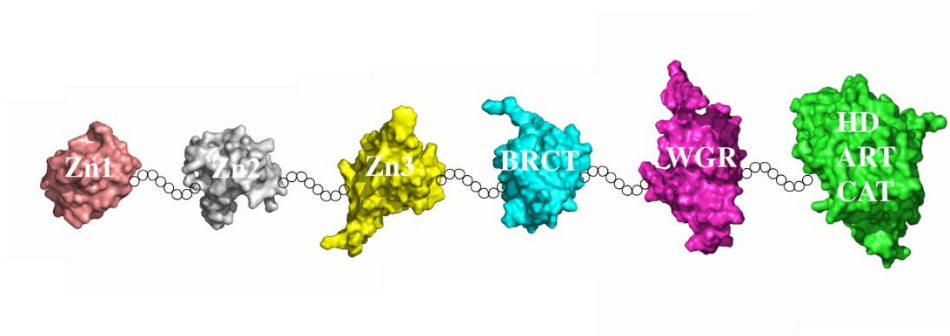

Fig. S5 Visualization of free PARP1 protein structure cited from Steffen et al.[30]

Table S5. Protein subunits properties based on the geometry of the first configuration from PDB entry.

Protein	Zinc finger 1	Zinc finger 2	Zinc finger 3	BRCA-1 C-terminus	Tryptophan-Glycine-Arginine	Catalytic domain

					domain	
Figure code	Zn1	Zn2	Zn3	BRCT	WGR	HD+ART+CAT
PDB code	3ODA	3ODE	2JVN	2COK	2CR9	1A26
Hydrodynamic radius [A]	17.75	18.19	21.31	19.41	23.65	28.78

Table S6. Linker center to center lenghts l_i

linker	3ODA 3ODE	3ODE 2JVN	2JVN 2COK	2COK 2CR9	2CR9 1A26
l_i [A]	103.9	154.5	144.72	158.06	120.95

The linkers are modeled with modified FENE potential

$$V = \begin{cases} 0 & r_i \le l_i \\ \frac{k r_m^2}{2} log\left[1 - \left(\frac{r_i - l_i}{r_m}\right)^2\right] & |r_i| > l_i \end{cases} \quad \text{(S1)}$$

where r_i is the distance between the spheres, r_m is the maximum stretch and k is the interaction potential. This is nonzero only if two spheres are further apart than l_i and allows for a stretch not larger than r_m. In simulations we set $r_m = 0.2a$ and $k = 1000k_BT$ to model an inextensible linker.

We normalize the length scale by the hydrodynamic diameter 2a of the smallest subunit (3ODA) and as a time scale the Brownian time $\tau_B = a^2/D$ with D being the diffusion coefficient of the sphere with diameter 2a. Using Brownian dynamics simulations with GRPY hydrodynamic interactions[32,33] from the calculated mean square displacement we find the diffusion coefficient of a single sphere, two spheres with a linker, and for the PARP1 protein model. All the files necessary to perform the calculations with the computer codes are available to download from https://github.com/pjzuk/GRPYlinked repository.

ESI8. Binding of PARP1 protein to RNA molecules

We performed an FCS experiment in PBS solution at 36˚C to determine if it is likely that the PARP1 protein can interact with RNA molecules (mRNA for cytoplasm). This measurement was based on mixing PARPi-FL inhibitor, PARP1 protein, and an RNA molecule of 2,000 nt. All components were at the same concentration. To avoid degradation of the RNA, measurements were performed under sterile conditions, and the entire experiment took no longer than 1.5 hours. As controls, we performed FCS measurements under the same conditions for: a) the inhibitor alone, b) the inhibitor with the PARP1 protein, and c) the inhibitor with the RNA molecule. The last control showed that the olaparib derivative does not bind to RNA (by comparing the diffusion coefficient for the inhibitor alone and PARPi-FL in solution with RNA).

FCS autocorrelation curves for the sample containing all three components (olaparib analog, PARP1 protein, and RNA molecule) were fitted with the normal three-component diffusion model. The first component of these curves was the freely diffusing inhibitor (diffusion time was fixed based on control a), the second component represented the olaparib analog – PARP1 protein complex (diffusion time was set based on control b), and the third component corresponded to the olaparib analog – PARP1 protein – RNA complex. From the obtained diffusion coefficient of the last component of the curves, the hydrodynamic radius was calculated, based on Equation 3. The parameters of the complex consisting of the inhibitor, PARP1 protein, and RNA are shown in Table S4. An example of obtained FCS autocorrelation curve is shown in Fig. S6.

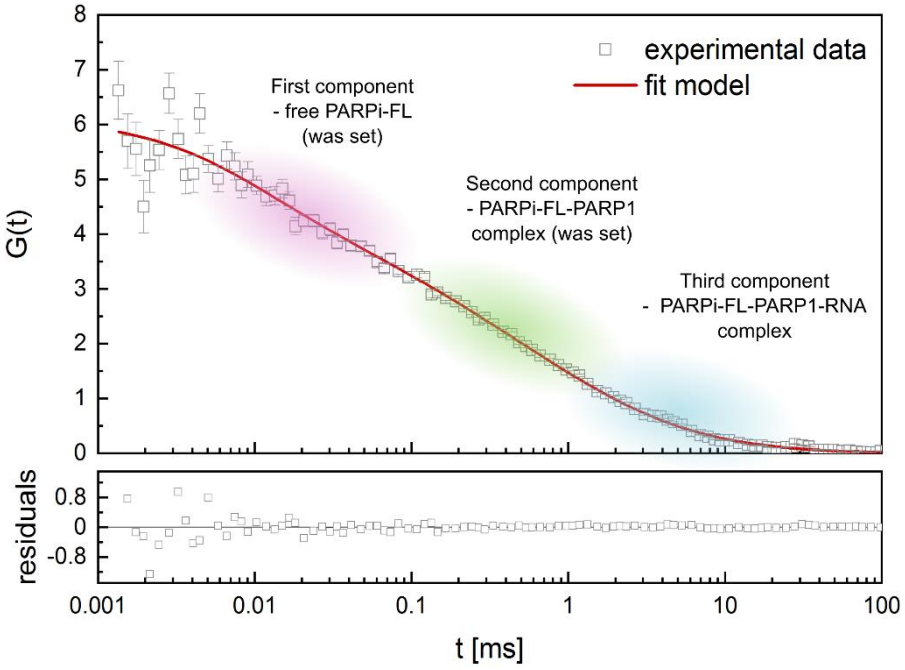

Fig. S6 FCS autocorrelation curve from the sample containing tested inhibitor, PARP1 protein, and RNA molecule with the three-component diffusion model fitted (Equation 1, when i=3). The bottom panel shows the residual curve.

ESI9. Component identification. Distribution of the third component of the MDA-MB-231 nucleus.

We identified three components in the nucleus of TNBC cells. The first one corresponded to freely diffusing PARPi-FL. The diffusion time of this component was not subject to fit and was determined from its hydrodynamic radius, nucleus nanoviscosity, and calibration data (confocal focus size). The second component was a complex of PARP1 protein and olaparib analog. It was identified by comparing the diffusion coefficient predicted from the viscosity curve and the coefficient obtained from fitting the experimental data. Analogously, the second component was precisely identified in the cytoplasm of MDA-MB-231 cells (Table S7).

Table S7. Summary of the diffusion coefficient of the PARP1 – olaparib analog complex predicted from the scale-dependent nanoviscosity model with the obtained one in MDA-MB-231 cells. Distinction based on cellular localization. Errors were calculated using total differential method (number of tested cells N = 10; each cell was measured three times).

Localization	Predicted diffusion coefficient [$\mu m^2/s$]	The obtained diffusion coefficient in MDA-MB-231 cells [$\mu m^2/s$]
Nucleus	9.10^4	8.60 ± 2.10
Cytoplasm	9.57 ± 2.19	8.10 ± 0.95

The third component of the nucleus of TNBC cells showed a wide range of diffusion coefficient values from 3.6 to 0.2 [$\mu m^2/s$]. Most likely, this component represents the interactions of the PARP1 protein with RNA molecules, which are known to have different sizes, ranging from long to very short molecules.[40] A plot of the distribution of diffusion coefficient values of the third component is shown in Fig. S7.

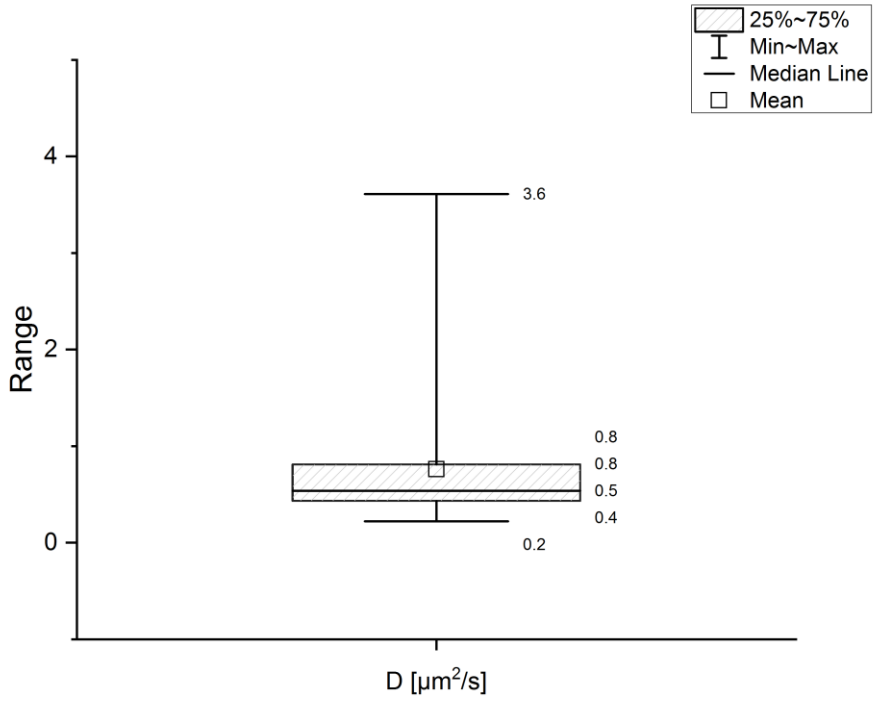

Fig. S7 Distribution of the third component of the FCS autocorrelation curve in the nucleus of MDA-MB-231 cells (number of tested cells N = 10; each cell was measured three times).